Augmented Lagrange Hopfield for Real Power Loss Minimization in Power Systems

Dieu Ngoc Vo, Hoang Khanh Cap Le, and Khai Phuc Nguyen

Abstract— *This paper proposes an augmented Lagrange Hopfield network (ALHN) for solving real loss minimization in power systems. The proposed ALHN is a conventional continuous Hopfield network with its energy function based on augmented Lagrange function. Moreover, the proposed method is a recurrent network with parallel processing which leads to fast convergence for large-scale problems. In the considered problem, the real power loss is determined using B-coefficients. The proposed method has been tested on the IEEE 14-bus, 30-bus, and 57-bus systems. The obtained results have indicated that the proposed ALHN can obtain better optimal solutions than particle swarm optimization (PSO) in a very fast manner. Therefore, the proposed ALHN can be implemented for solving the real power minimization problem in power systems.*

Keywords— **Augmented Lagrange Hopfield network, real power loss minimization, neural network, power flow.**

1. INTRODUCTION

In modern power systems, the improvement of operation has become more important due its contribution to the enhancement of power system efficiency. The minimization of real power losses in power systems is also very important because it can lead to a more economic operation of a power system. Once real power loss in power systems is minimized, the electric power is more efficiently consumed [1]. For real power loss minimization, the existing generation and transmission systems can be efficiently utilized without building new systems. Therefore, the objective of the real power loss minimization is to determine power generation of power plants so as the total real power loss in power systems is minimized to save cost of loss satisfying power constraint and generator limits.

Due to its importance, the problem of power loss minimization has been investigated by several researches [2-5]. In [2], the power loss in the system is calculated using B-coefficients and verified with traditional RI^2 or differential power methods based on the solution of power flow by Newton-Raphson method. In the proposed method, the voltage control using capacitor bank or transformer tap changer will be done to improve voltage level while power loss minimized. In [3], a hybrid particle swarm optimization is implemented for loss reduction study. The proposed application in this paper is the use of a developed optimal power flow based on loss minimization function including two steps. The first is to determine the critical area of the power system under the point of view of voltage instability, and the second is to calculate the amount of shunt reactive power compensation that takes place in each bus by particle swarm optimization method. In [4], meta-heuristic search methods such as bacteria foraging algorithm, conventional algorithm, and differential genetic algorithm have been implemented for transmission loss minimization. The active loss minimization problem has been solved by a predictor–corrector modified barrier approach. In this proposed approach, the inequality problem constraints are transformed into equalities by introducing positive auxiliary variables perturbed by the barrier parameter and treated by the modified barrier method.

In this paper, an augmented Lagrange Hopfield network (ALHN) is proposed for solving real loss minimization in power systems. The proposed ALHN is a conventional continuous Hopfield network with its energy function based on augmented Lagrange function. Moreover, the proposed method is a recurrent network with parallel processing which leads to fast convergence for large-scale problems. In the considered problem, the real power loss is determined using B-coefficients. The proposed method has been tested on the IEEE 14-bus, 30-bus, and 57-bus systems. The obtained results are compared to those particle swarm optimization method.

2. PROBLEM FORMULATION

Mathematically, the real power loss minimization is formulation as follows:

The objective is to minimize total real power loss:

$$\text{Min } P_{loss} \tag{1}$$

subject to:

- Real power balance

$$\sum_{i=1}^{N} P_{gi} = P_D + P_{loss} \tag{2}$$

- Ramp rate constraint

The authors are with Department of Power Systems, Ho Chi Minh City University of Technology, 268 Ly Thuong Kiet str., 10th dist., HCMC, Vietnam. Email: vndieu@hcmut.edu.vn (D.N. Vo).

$$P_{gi} - P_{gi}^0 \le UR_i \text{ , as power increases} \quad (3)$$

$$P_{gi}^0 - P_{gi} \le DR_i \text{ , as power decreases}$$

(4)

- Generator limits

$$P_{gi,\min} \le P_{gi} \le P_{gi,\max} \quad (5)$$

where

- N : number of generators
- P_{loss} : total real power loss
- P_{gi} : real power output of generator i
- $P_{gi,max}$: maximum real power output of generator i
- $P_{gi,min}$: minimum real power output of generator i
- P^0_{gi} : initial real power output of generator i
- P_D : total power system demand

3. AUGMENTED LAGRANGE HOPFIELD NETWORK IMPLEMENTATION

For implementation in ALHN, the real power loss in (1) is calculated using Kron's formula [6]:

$$P_{loss} = \sum_{i=1}^{N}\sum_{j=1}^{N} P_{gi} B_{ij} P_{gj} + \sum_{i=1}^{N} B_{0i} P_{gi} + B_{00} \quad (6)$$

where B_{ij}, B_{0i}, and B_{00} are the B-coefficients for real power loss.

The augmented Lagrange function is formulated for the problem:

$$L = \sum_{i=1}^{N}\sum_{j=1}^{N} P_{gi} B_{ij} P_{gj} + \sum_{i=1}^{N} B_{0i} P_{gi} + B_{00} + \lambda\left(P_D + P_{loss} - \sum_{i=1}^{N} P_{gi}\right) + \frac{1}{2}\beta\left(P_D + P_{loss} - \sum_{i=1}^{N} P_{gi}\right)^2 \quad (7)$$

where λ and β are Lagrange multiplier and penalty factor, respectively.

The energy function of ALHN is formulated based on the augmented Lagrange function as follows:

$$E = \sum_{i=1}^{N}\sum_{j=1}^{N} V_{gi} B_{ij} V_{gj} + \sum_{i=1}^{N} B_{0i} V_{gi} + B_{00} + V_\lambda\left(P_D + P_{loss} - \sum_{i=1}^{N} V_{gi}\right) + \frac{1}{2}\beta\left(P_D + P_{loss} - \sum_{i=1}^{N} V_{gi}\right)^2 + \int_0^{V_{gi}} g^{-1}(V)\,dV \quad (8)$$

where V_{gi} is the output of continuous neuron i representing power output P_{gi} of generator i, V_λ is the output of the multiplier neuron representing the Lagrange multiplier λ, and $g^{-1}(V)$ is the inverse function of sigmoid function of continuous neurons.

In (8), the sums of integral terms are Hopfield terms where their global effect is a displacement of solutions toward the interior of the state space [7].

The dynamics of the neurons are defined by:

$$\frac{dU_{gi}}{dt} = -\frac{\partial E}{\partial V_{gi}} = -\left\{\left(\sum_{j=1}^{N} 2B_{ij}P_{gi} + B_{0i}\right) + \left[V_\lambda + \beta\left(P_D + P_{loss} - \sum_{i=1}^{N} V_{gi}\right)\right] \times \left[\left(\sum_{j=1}^{N} 2B_{ij}P_{gi} + B_{0i}\right) - 1\right] + U_{gi}\right\} \quad (9)$$

$$\frac{dU_\lambda}{dt} = +\frac{\partial E}{\partial V_\lambda} = P_D + P_{loss} - \sum_{i=1}^{N} P_{gi} \quad (10)$$

where U_{gi} and U_λ are the inputs of continuous and multiplier neurons, respectively.

The inputs of neurons at iteration n are updated by:

$$U_{gi}^{(n)} = U_{gi}^{(n-1)} - \alpha_i \frac{\partial E}{\partial V_{gi}} \quad (11)$$

$$U_\lambda^{(n)} = U_\lambda^{(n-1)} + \alpha_\lambda \frac{\partial E}{\partial V_\lambda} \quad (12)$$

where α_i and α_λ are updating step size of continuous and multiplier neurons, respectively.

The outputs of continuous neurons are calculated using a sigmoid function:

$$V_{gi} = g(U_{gi}) = \left(\frac{P_{gi,high} - P_{gi,low}}{2}\right)[1 + \tanh(\sigma U_{gi})] + P_{gi,low} \quad (13)$$

where

$$P_{i,high} = \min\left\{P_{gi,\max}, P_{gi}^0 + UR_i\right\} \quad (14)$$

$$P_{i,low} = \max\left\{P_{gi,\min}, P_{gi}^0 - DR_i\right\} \quad (15)$$

The output of the multiplier neuron is calculated using a transfer function:

$$V_\lambda = g(U_\lambda) = U_\lambda \quad (16)$$

Selection of parameters

In the ALHN, the parameters have to be predetermined including sigmoid function slope, updating step sizes for neurons and penalty factors for augmented Lagrange function. By experiments, the values of sigmoid function slope and penalty factors are fixed at 100 and 0.001, respectively. The values of the others will vary depending on the data of considered problem. It is observed that the larger the value of updating step sizes the closer the discrete system behavior, producing values at the upper and lower limits of each neuron. On the contrary, the smaller the value of updating step sizes the slower convergence of the network.

Initialization

In the proposed ALHN, all neurons need to be initialized. For the continuous neurons, their initial outputs are determined:

$$V_{gi}^{(0)} = P_D \frac{P_{gi,\max}}{\sum_{i=1}^{N} P_{gi,\max}} \quad (17)$$

and the output of the multiplier neuron is initialized by:

$$V_{\lambda}^{(0)} = -\frac{\sum_{j=1}^{N} 2B_{ij}P_{gj} + B_{0i}}{\sum_{j=1}^{N} 2B_{ij}P_{gj} + B_{0i} - 1} \quad (18)$$

The inputs of all neurons are determined based on their outputs using the inverse function of sigmoid function for continuous neurons and transfer function for the multiplier neuron.

The proof of convergence and the explanation of the proposed ALHN method are given in [8].

Stopping criteria

The algorithm of ALHN will be terminated when either the maximum error Err_{max} including constraint error and iterative error is lower than a pre-specified tolerance ε or maximum number of iterations N_{max} is reached.

Overall procedure

Overall algorithm of ALHN for solving the problem is as follows:

Step 1: Solve power flow problem by Newton-Raphson to determine B-coefficients.

Step 2: Select parameters for the neural network.

Step 3: Initialize outputs of all neurons and calculate their corresponding inputs.

Step 4: Set n = 1.

Step 5: Calculate dynamics of neurons using (9)-(10).

Step 6: Update inputs of neurons using (11), (12).

Step 7: Calculate corresponding outputs of neurons using (13) and (16).

Step 8: Solve power flow problem by Newton-Raphson to determine B-coefficients

Step 7: If $Err_{max} > \varepsilon$ and n < N_{max}, $n = n + 1$ and return to Step 4. Otherwise, stop.

4. NUMERICAL RESULTS

The proposed ALHN has been tested on the IEEE 14-bus, 30-bus, and 57-bus systems. The data for these test systems are given in [9-10]. For result comparison, the PSO method [11] has been also implemented for solving these systems. The algorithms of the methods are coded in Matlab and run on a 1.6 GHz Intel PC. For obtaining power flow solution, the Matpower toolbox [10] has been used. For stopping criteria of the ALHN algorithm, the maximum error and maximum number of iterations are set to 10^{-3} and 2500, respectively.

The IEEE 14-bus system: The system includes 14 buses and 20 branches, in which there five generation buses and three transformer branches. The total real power demand of the system is 259 MW. The diagram of this system is given in Appendix. The result comparison from ALHN and PSO is given in Table 1 and the energy characteristic of the ALHN for the system is given in Fig. 1.

The IEEE 30-bus system: The system includes 30 buses and 41 branches, in which there six generation buses and four transformer branches. The total real power demand of the system is 283.4 MW. The diagram of this system is given in Appendix. The result comparison from ALHN and PSO is given in Table 2 and the energy characteristic of the ALHN for the system is given in Fig. 2.

Table 1. Result comparison for the IEEE 14-bus system

			ALHN	PSO
Bus	$P_{i,min}$ (MW)	$P_{i,max}$ (MW)	P_i (MW)	P_i (MW)
1	50	200	67.0495	97.5839
2	20	80	80	64.1423
3	15	50	50	43.8667
6	10	30	30	26.0951
8	10	35	35	31.2324
P_L (MW)			3.0486	3.9204
CPU (s)			0.75	4.79

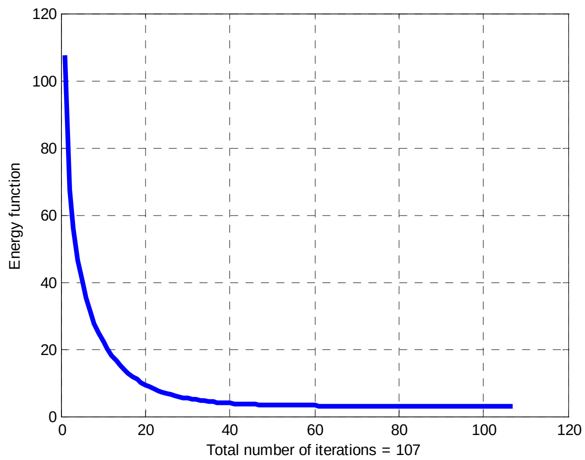

Fig. 1. Energy function of ALHN for the IEEE 14-bus system.

Table 2. Result comparison for the IEEE 30-bus system

			ALHN	PSO
Bus	$P_{i,min}$ (MW)	$P_{i,max}$ (MW)	P_i (MW)	P_i (MW)
1	50	200	51.9894	95.9628
2	20	80	80	60.8501
5	15	50	50	48.3410
8	10	35	35	30.0364
11	10	30	30	25.5737
13	20	40	40	27.2553
P_L (MW)			3.5886	4.6193
CPU (s)			1.14	5.60

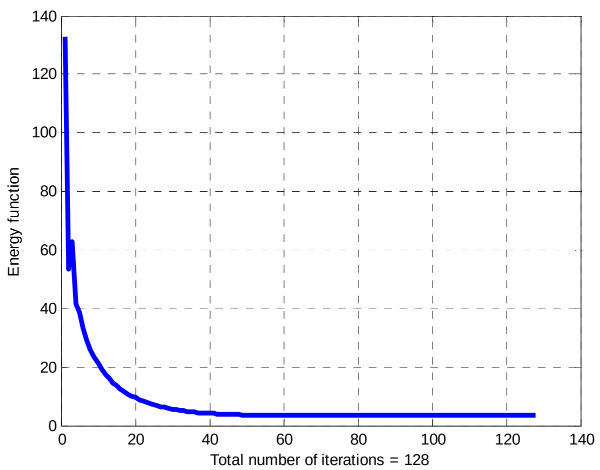

Fig. 2. Energy function of ALHN for the IEEE 30-bus system.

The IEEE 57-bus system: The system includes 57 buses and 80 branches, in which there seven generation buses and fifteen transformer branches. The total real power demand of the system is 1250.8 MW. The diagram of this system is given in Appendix. The result comparison from ALHN and PSO is given in Table 3 and the energy characteristic of the ALHN for the system is given in Fig. 3.

Based on the result comparison given in Tables 1, 2, and 3, the proposed ALHN can obtain better solutions than the PSO method for the all test systems. Moreover, the proposed ALHN also obtain the solutions much faster than the PSO method for all systems. Therefore, the proposed ALHN is more efficient than the PSO method for solving the problem.

Table 3. Result comparison for the IEEE 57-bus system

			ALHN	PSO
Bus	$P_{i,min}$ (MW)	$P_{i,max}$ (MW)	P_i (MW)	P_i (MW)
1	200	600	200	212.9463
2	30	150	30	30
3	30	140	107.2187	96.2084
6	20	100	99.9528	100
8	120	550	266.5468	264.5912
9	20	150	150	150
12	100	410	410	410
P_L (MW)			12.9175	12.9458
CPU (s)			2.46	6.93

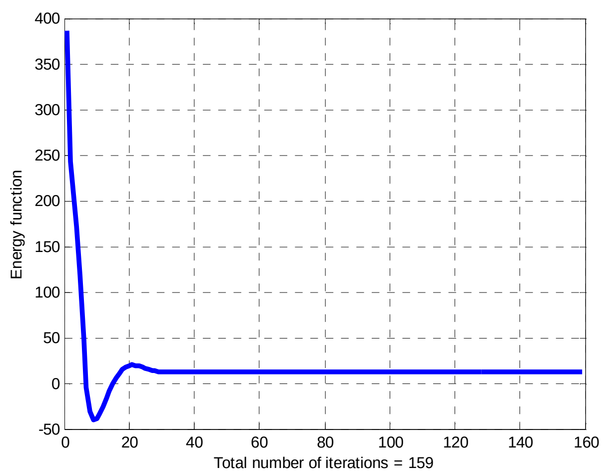

Fig. 3. Energy function of ALHN for the IEEE 14-bus system.

5. CONCLUSION

In this paper, the ALHN has been efficiently implemented for solving the real power loss minimization problem in power systems. The ALHN method is a simple and very easy implementation on optimization problems in power systems. The proposed uses augmented Lagrange function for handling equality constraints of the problem while the sigmoid function of continuous neurons can properly handle inequality constraints of the problem. In addition, the ALHN method is based on the parallel processing of neural network which leads to very fast convergence. The proposed ALHN has been tested on the IEEE 14-bus, 30-bus, and 57-bus systems and the obtained results have indicated that the proposed ALHN is more efficient than PSO in terms of total power loss and computational time. Therefore, the proposed ALHN could be applicable for solving the real power loss minimization in power systems.

REFERENCES

[1] Lukman, D., Blackburn, T.R. and Walshe, K. (2000). Loss minimization in industrial power system operation. *Proc. of the Australasian Universities Power Engineering Conference (AUPEC'94)*, Brisbane, Australia.

[2] Lukman, D. and Blackburn, T.R. (2001). Modified algorithm of load flow simulation for loss minimization in power systems. *Proc. of the Australasian Universities Power Engineering Conference (AUPEC-2001)*, Perth, Australia.

[3] Esmin, A..A.A, Lambert-Torres, G., and de Souza, A.C.Z. 2005. A hybrid particle swarm optimization applied to loss power minimization. *IEEE Trans. Power Systems*, 20(2): 859-866.

[4] Mishra, S., Redely, G.D., Rao, P.E. and Santosh, K. (2007). Implementation of new evolutionary techniques for transmission loss reduction. *IEEE Congress on Evolutionary Computation* (CEC 2007), Singapore.

[5] de Sousaa, V.A., Baptistab, E.C., and da Costa, G.R.M. 2009. Loss minimization by the predictor–corrector modified barrier approach. *Electric Power Systems Research*, 79 (5): 803-808.

[6] Wood, A.J. and Wollenberg, B.F. 1996. Power system generation, operation and control, 2nd ed., New York: John Wiley.

[7] van den Berg, J. and Bioch, J.C. (1993). Constrained optimization with a continuous Hopfield-Lagrange model. Technical report EUR-CS-93-10, Erasmus University Rotterdam, Comp. Sc. Dept., Faculty of Economics.

[8] Dieu, V. N. and Ongsakul, W. 2006. Enhanced augmented Lagrangian Hopfield network for unit commitment. *IEE Proc. Generat. Transm. Distrib.*, 153(6): 624-632.

[9] Dabbagchi, I. and Christie, R. (1993). Power systems test case archive. *University of Washington*. Retrieved Feb. 20, 2011, from http://www.ee.washington.edu/research/pstca/.

[10] Zimmerman, R.D.; Murillo-Sánchez; C.E. and Thomas, R.J. (2011). MATPOWER steady-state operations, planning and analysis tools for power systems research and education. *IEEE Trans. Power Systems*, 26(1): 12-19.

[11] Kennedy, J. and Eberhart, R. (1995). Particle swarm optimization. *Proc. IEEE Conf. Neural Networks* (ICNN'95), Perth, Australia, vol. IV: 1942-1948.

APPENDIX

The diagram of the IEEE 14-bus, 30-bus and 57-bus systems are given in Figs. 4, 5, and 6, respectively.

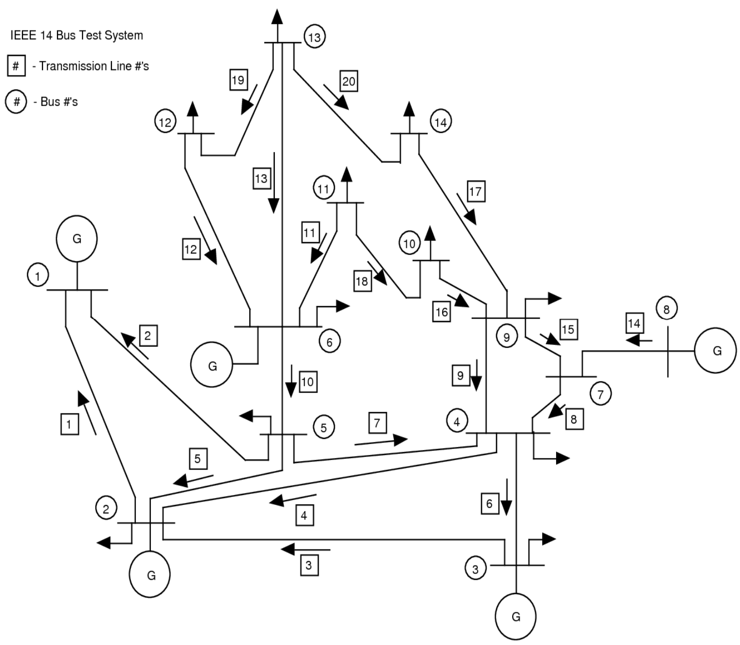

Fig. 4. The IEEE 14-bus system.

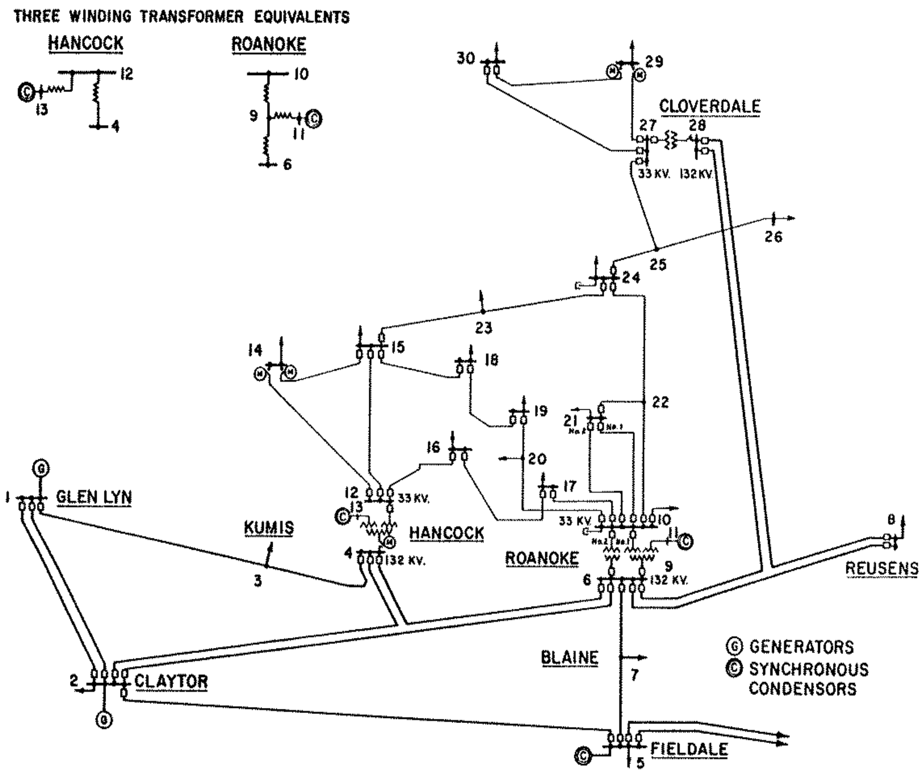

Fig. 5. The IEEE 30-bus system.

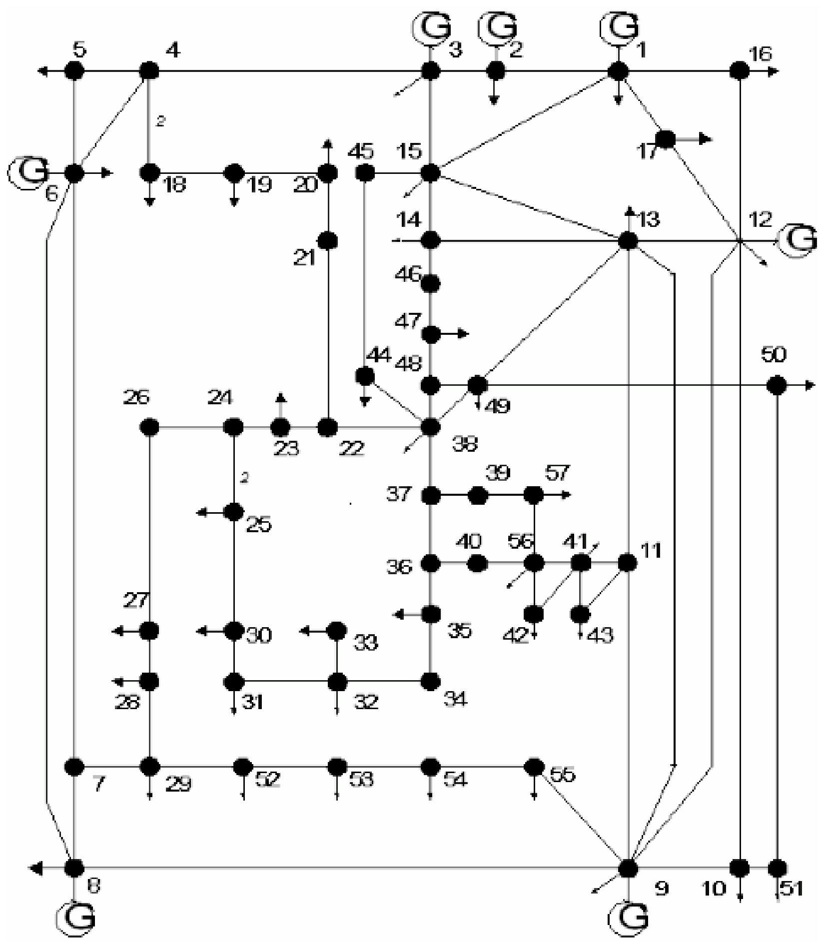

Fig. 6. The IEEE 57-bus system.